A Space-Based CCD Experiment for High-Precision Astrometry

S. Shaklan and S. Pravdo
Jet Propulsion Laboratory
California Institute of Technology
4800 Oak Grove Drive
M/S T1701
Pasadena, CA 91109

ABSTRACT

The Astrometric Imaging Telescope, an orbiting 1.5 m low-distortion Ritchey-Chretien, will use a large format CCD to record star trails as the CCD is dragged across the image plane. Star-trail separations, when averaged over thousands of pixels, yield photon-noise limited centroids with 10 micro-arcsecond accuracy. In this paper, we will discuss the important CCD and optical design parameters that affect astrometric accuracy. For the CCD, these include charge transfer efficiency, pixel-to-pixel relative quantum efficiency, sub-pixel QE gradients, and systematic pixel dislocations. For optical design, they are tolerancing of parameters such as secondary mirror decenter and tilt, and conic constants. We present a point design for a system that can achieve 10 micro-arcsecond accuracy over a long-term mission. End-to-end modeling, including high precision diffraction calculations, is used to validate the design.

1 INTRODUCTION

The Astrometric Imaging Telescope (AIT) is a proposed orbiting 1.5 m diameter Ritchey-Chretien telescope[1,2]. Its primary mission is to detect extra-solar Jupiter and Uranus-like planets using both a coronagraph for direct imaging and relative astrometry for indirect measurement. This paper addresses results of end-to-end modeling of the astrometric portion of the mission.

The astrometric instrument consists of the two-mirror telescope and a large format CCD that is dragged across the focal plane. No other optics are required. The instrument operates by pointing at a field of stars, then dragging the chip across the image plane obliquely to the CCD rows. Star trail separation indicates the relative stellar positions in one dimension. The telescope is rotated and the experiment repeated to obtain the perpendicular dimension. Each column along the star trail provides an independent measurement of position. The reason for star trails, rather than conventional direct imaging, is to average over the random errors that can occur in each column, *e.g.* quantum efficiency (QE) fluctuations, sub-pixel QE gradients, and pixel positional offsets. Also, a star trail collects independent measurements in one image, minimizing the amount of data to be downlinked.

In this paper we briefly describe the end-to-end modeling; a more thorough discussion is given elsewhere[3]. We then discuss the CCD model and specify tolerances on the random errors just noted. We then present a point design for the telescope that satisfies astrometric performance requirements as well as opto-mechanical constraints. Tolerance on the optical design, based upon end-to-end modeling of simulated representative star fields, is presented. Finally, the model is used to determine integration times for typical fields.

2 END-TO-END MODEL

Our model consists of several simulated star fields representing a uniform sampling of the sky, a ray-trace/diffraction program, the CCD model, a photon noise generator, and an astrometric analysis program. All software is executed on a Sun Sparc 2 workstation.

2.1 Imaging code

End-to-end modeling begins with a high-precision optical ray-trace and diffraction program called the Controlled Optics Modeling Package (COMP)[4].

0-8194-1181-7/93/$6.00

COMP is a flexible program that is implemented in either a stand-alone mode or as a library of subroutines callable from a FORTRAN program. A star from the field is selected, COMP then reads a file containing the optical prescription, and rays are traced from the field point through the system to the focal plane. The monochromatic diffraction (and/or aberration) limited point spread function is then computed. Modification of the prescription facilitates a study of the opto-mechanical tolerances without any modification to the code.

Since AIT is designed to have a precision of 10 micro-arcseconds (5 x 10^{-11} radians), the code itself must be understood and accurate at the micro-arcsecond level. COMP's ray trace is known to be accurate to nano-arcseconds. In theory, the diffraction limited image should have the same centroid as a bundle of rays traced through the system[5]. We find that, to a linear magnification term, diffraction centroids match ray centroids to within a few micro-arcseconds across the field. The linear magnification term is inconsequential since it is removed by the affine transformation described below. A more detailed description of the code's precision is given elsewhere[3].

For these simulations, a total of 1840 rays were traced through the telescope. Diffraction images were computed on a 512 x 512 grid with a pixel size of 0.75 μm.

2.2 CCD model

The CCD is assumed to be a flat detector with uniformly spaced pixels and a 100% fill factor. Each pixel is assigned a QE that includes a random term chosen from a Gaussian distribution, and linear sub-pixel QE gradient. The chip as a whole is assumed to have a uniform Charge Transfer Efficiency (CTE) with 0.999<CTE<1.

While a real CCD may have a non-zero power spectrum that continues beyond linear sub-pixel gradients, these are inconsequential for centroiding. Since the image has mainly a linear component across the pixels, parabolic and higher order gradients don't affect the centroids. Additionally, because the images are dragged obliquely across the pixels, pixel gradient averaging occurs and higher order terms are quickly reduced.

The CCD chosen is available as a standard item from Loral[6]. It is a 4096 x 4096 chip with 7.5 micron pixels. With the current design, this provides a 4.5 arcminute diameter field-of-view. AIT will actually use two identical chips mounted side-by-side. This allows simultaneous measurement of all stars as they are dragged across the field. Simultanaeity is required in order to reduce spacecraft jitter noise on the centroids.

2.3 Astrometric model

AIT performs relative astrometry, measuring the motion of a target star relative to a background frame. Over its lifetime, it will measure each target star several times per year. With each subsequent observation, the pointing, roll, focus, focal plane position, and optical components will change at some small level. The reference stars allow one to make an affine transformation between frames. We have found that a 3 term linear model is more sensitive to aberrations. Instead, we use a 6 term quadratic model given by

$$x' = a_o + a_1 x + a_2 y + a_3 xy + a_4 x^2 + a_5 y^2 \quad (1)$$

where x and y are the coordinates of a star in the original frame, and x' is the coordinate in subsequent frames. y' is measured in separate observations. A least squares routine is used to perform the affine transformation. Each star is weighted according to its brightness and image quality. At least 6 reference stars are required for the model. Error propagation is described below.

3 OPTICAL DESIGN

The ideal astrometric telescope has zero distortion and forms perfectly symmetric images across the field-of-view. No two-mirror design can achieve this, but a special class of Ritchey-Chretien designs can eliminate third order distortion, spherical aberration, and coma, while maintaining a reasonably flat field. The equations for determining this design have been given by Korsch[7]. The AIT design is driven by additional factors, such as the desire for a

Table 1: AIT Design Parameters

Parameter	Value
Primary diameter	1.50 m
Primary focal length	7.48 m
Primary conic constant	-1.0787
Secondary diameter	0.44 m
Secondary focal length	-2.96 m
Secondary conic constant	-4.9381
Primary-secondary separation	5.50 m
Back-focal distance	0.50 m
System focal length	22.64 m

small secondary mirror to reduce sidelobes for the coronagraph, constrained overall length, and the need for a large collecting area.

Two acceptable designs exist: both have 1.5 m diameter primary mirrors and an overall length of 6 m. The first has the entrance pupil at the primary mirror. This requires a 73 cm diameter secondary mirror, with a system focal length of 13 m. The low magnification of the secondary mirror is advantageous in terms of decenter and tilt tolerances, but this is outweighed by the disadvantages of a large secondary (increased sidelobes and integration time) and short focal length (demanding smaller pixels, which have smaller full-well capacities).

The second design has the entrance pupil located in the plane of the secondary mirror. Design parameters are given in Table I. With this design, the plate scale is 68 milli-arcseconds per 7.5 micron pixel, while the diffraction limited full-width of the central lobe is 168 milli-arcseconds. 2.47 pixels

The telescope maintains diffraction limited performance across the 4.5 arcminute field-of-view. The Strehl ratio is 0.994 at the edge of the field.

Figure 1 shows the distortion across the field-of-view for this design. Total distortion is a few micro-arcseconds. It can be seen that the distortion actually measured on the CCD closely follows the diffraction and ray-centroid distortions.

4 CENTROIDING ON A CCD

We have considered two methods for determining image centroids. First, one can use the standard centroid estimator, given by

$$c = \frac{\Sigma_p p I_p}{\Sigma_p p} \tag{2}$$

where p is the pixel value and I_p is the intensity at that pixel. This estimator is extremely sensitive to both positioning of the image with respect to pixels, as well as to the number of rows used in the estimation. The second method is a matched filter With a properly generated filter, the centroid estimate is completely insensitive to the number of rows and relative image/pixel positioning.

From previous work on image centration using Ronchi rulings[3], we have seen that true image centroids are well behaved even in the presence of optical perturbations, while estimators that do not measure the true centroid (such as an improperly formed matched filter) are not so robust. For this reason, we use the standard centroid estimator in this work. Matched filter performance is roughly the same in terms of sensitivity to pixel errors and pixel gradients, but it is 3 times more light efficient.

4.1 Standard centroid estimate

The centroid estimate is formed from a swath 11 rows (0.75 arcseconds) wide, centered on the peak of the image. As the image moves within the central pixel, the apparent centroid error is of order 0.01 pixels. By dragging the

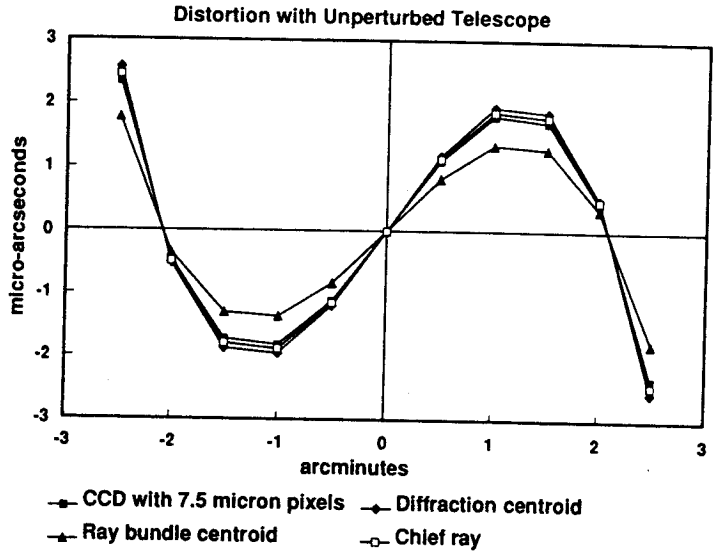

Figure 1: Distortion in the unperturbed AIT. Chief ray distortion is the classical 3rd order aberration. Ray-centroid distortion is based upon the centroid of 1840 rays traced through the telescope. Diffraction distortion is based upon the centroid of the diffraction-limited image, formed on a high-resolution grid. The CCD curve shows distortion measured on 7.5 micron pixels.

image obliquely across the pixels, this error is averaged to a negligible value. To simulate this, we compute the centroid as it shifts 0.1 pixels, then average the results after shifting by a full pixel. Residual shift at the end of the scan are of order $0.01/4096 = 2 \times 10^{-6}$ pixels $<<$ 1 micro-arcsecond.

Over the years in space, contamination may lead to small changes in the relative pixel QE. For a QE standard deviation σ_{QE} per pixel, we find that the centroid error in each column has a standard deviation given by

$$\sigma_{c,QE} = 9000\sigma_{QE} \quad \text{micro} - \text{arcseconds}. \tag{3}$$

Assuming that QE errors are uncorrelated and white, we require

$$N_{QE} = \left(\frac{\sigma_{c,QE}}{10 \ \text{micro} - \text{arcsec}} \right)^2 \tag{4}$$

pixels to average the centroid error to 10 micro-arcseconds. For 1% QE errors, only 81 columns are needed. For 4096 columns, we can tolerate QE errors of 7%. This should be trivial to obtain using a flat-field source on board the spacecraft.

For sub-pixel gradients, the centroid standard deviation is given by

$$\sigma_{c,gr} = 1710\sigma_{gr} \quad \text{micro} - \text{arcseconds}. \tag{5}$$

Assuming white, uncorrelated gradients having a standard deviation of σ_{gr}=0.1, 294 columns are required to average the error to 10 micro-arcseconds.

The number of photons required is determined by the image width. For the telescope and CCD parameters given above, we find that 5.5×10^7 photons reduce the photon-limited centroid error to 10 micro-arcseconds.

Table 2: AIT Tolerancing

Perturbation	Tolerance
Secondary decenter	$\pm 500\ \mu$m
Secondary tilt	$\pm$ 1.0 arcminutes
Secondary conic constant	$> \pm$ 0.005
Primary conic constant	$> \pm$ 0.01
Secondary-primary separation	$> \pm$ 1 mm

4.2 Charge transfer efficiency

After several years in low earth orbit, radiation, particularly proton bombardment, causes deterioration of CCD charge transfer efficiency (CTE). Data from laboratory radiation shows that the CTE loss has components that are both proportional to and independent of signal strength[8].

Here we consider vertical (columnar) CTE losses. These are roughly perpendicular to star trails and have a much more severe effect than horizonal losses. Vertical CTE induces a vertical tail on the star trail. This biases the centroid away from the horizonal shift register (HSR). Star trails near the HSR are less affected than those near the other side of the chip.

We have written a simple algorithm to simulate the star trail profile for a given CTE, for proportional CTE loss (which is signal-independent). The profiles are then used in our standard centroid estimator algorithm to yield the following equation for centroid shift S vs. CTE and the number of pixels N_p from the HSR:

$$S = N_p(1 - \mathrm{CTE})6605 \quad \mathrm{micro-arcseconds}. \tag{6}$$

The equation holds for (1-CTE)$< 10^{-3}$.

For an absolute tolerance of 10 micro-arcseconds at the largest field point ($N_p = 4096$), a CTE > 0.99999963 is required. However, the CTE effect is *linear* in field (linear in N_p); it is completely removed by the affine transformation described above. Our CTE tolerance, in fact, is very loose. Even shifts of a milli-arcsecond (CTE = 0.999963) do not adversely affect the astrometry. With proper shielding, CTE should remain above this level for the mission lifetime. The Cassini CCD is expected to maintain CTE > 0.99996 in a harser environment[9].

5 OPTICAL TOLERANCING

Any aberration that introduces coma or distortion affects the astrometric accuracy at the center of the field. With our end-to-end model, we can easily modify the optical prescription and determine how much modification leads to unacceptable accuracy. First, we determine centroids (as measured by the CCD) for a field of stars and an unperturbed telescope. We then perturb the optical prescription and shift the field by 2 arcseconds while rotating it by 1 degree (thus simulating a slight mispointing and roll of the telescope). We re-analyze the field and fit an affine transformation to the two observations. The apparent motion of the center of the field indicates the astrometric error caused by the perturbation. Figure 2 shows the distortion when the secondary is laterally displaced by 100 microns. The figure shows that while the "true" centroids are not affected (except by a field- independent shift that has been removed), the centroid measured on the CCD is slightly shifted.

Table II lists the perturbations and tolerances that we have studied. In addition to these, we plan to introduce contamination and random phase errors on the mirror surfaces.

These tolerance values indicate a worst-case scenario, where it is impossible to determine the aberrations (or, equivalently, the perturbations) in the system. However, preliminary tests show that improvements of between 2-5 are possible by making multiple shifted images of a star cluster with a few bright stars and calibrating the differential image motions.

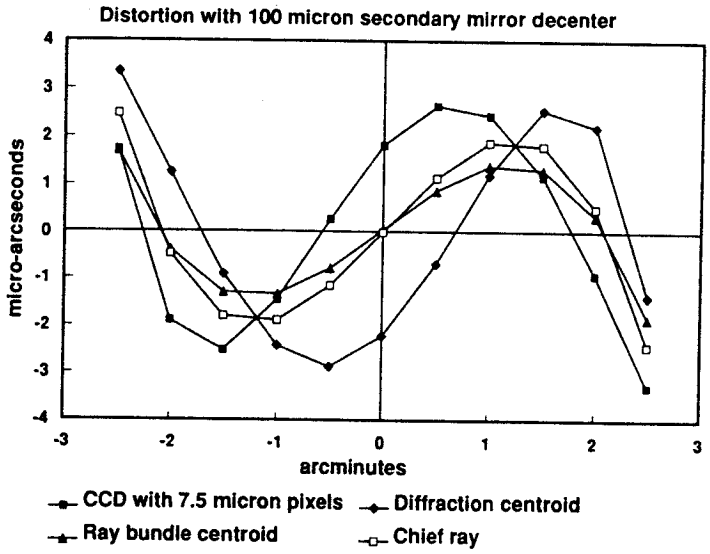

Figure 2: Distortion when the secondary mirror is laterally displaced by 0.1 mm. The CCD centroid shift is due to an interaction between binning on 7.5 micron pixels, design astigmatism, and field independent coma caused by the secondary displacement.

6 INTEGRATION TIME

We have simulated 33 star fields representing a random sampling of the sky. Only those fields having 6 or more stars brighter than m_v=17 are considered; the signal-to-noise ratio of fainter stars is limited by CCD read noise. There is a 70% probability of obtaining such a field.

Each field is run through the end-to-end model twice. The first time, star positions are computed without any photon noise. The second time, a 1 second integration is assumed. The affine transformation is then applied to the two observations. The formal least-squares error on motion of the center of the field is used to estimate the astrometric error in one second of integration. It is then trivial to compute the time required to reduce the astrometric error to 10 micro-arcseconds. We assume a total optical bandwidth of 500 $\pm$ 200 nm, and average throughput (including QE) of 25%.

Of the 33 fields, one field requires an integration time that is 50 times the standard deviation of the remaining fields. The large integration time is due to the particular stellar intensity and spatial distributions. For the remaining 32 fields, the average integration time is 5000 seconds to obtain 10 micro-arcsecond precision at the target star. The standard deviation is also 5000 seconds. Table III gives a histogram of integration times. For the brightest 24 fields, representing 50% of available target stars, the average integration time is 2540 seconds.

We note that integration times can be improved by 1) increasing the diameter of the primary; 2) decreasing pixel size; 3) increasing the field of view; 4) using a matched filter for centroiding; and 5) using a linear affine model. Option 1 is unlikely because of the physical limitations of the launch fairing. Option 2 would decrease the full well capacity and dynamic range of the CCD. Options 3 and 4 have the disadvantage of rendering the telescope more sensitive to opto-mechanical perturbations, The linear model decreases average integration times to 650 seconds and offers a "no-cost" improvement if on-orbit conditions (alignment of the optics) allow it.

Table 3: Histogram of Integration Times

Integration Time (sec)	Number of fields
< 1000	6
< 2000	13
< 3000	15
< 4000	17
< 5000	21
< 6000	23
< 12000	27

7 CONCLUSION

Our end-to-end modeling indicates that an astrometric telescope with a large-format CCD can achieve the required measurement accuracy. CCD calibration of a few percent per pixel, easily achieved in flight, is all that is required for averaging random QE errors. Vertical CTE changes induce a linear magnification that is completely removed by the affine transformation. Optical perturbations of 500 microns and 1 arcminute are permitted on the secondary. Typical integration times are about 45 minutes. The point design appears to be robust and efficient enough to serve as the basis for a long-term astrometric program.

Our modeling effort will continue to improve. We plan to model mirror contamination, random mirror phase errors, and spacecraft jitter. The improved model will also include multiple wavelength diffraction computations. We are also investigating the behavior of the affine transformation as a function of the light distribution in the reference frame.

8 ACKNOWLEDGEMENTS

The Korsch-based optical design was optimized by H. Kadogawa. We acknowledge E. Levy, R. Terrile, A. Buffington, A. Nonnenmacher, K. Shu, C. Ftaclas, and G. Gatewood for participating in this work. This work was carried out at the Jet Propulsion Laboratory, California Institute of Technology, under contract with the National Aeronautics and Space Administration.

9 REFERENCES

1. S. Pravdo, *et al.*, "The Astrometric Imaging Telescope: Detection of Planetary Systems with Imaging and Astrometry," submitted to *Astrophys. and Space Sci.*,, 1993.

2. S. Pravdo, "The Astrometric Imaging Telescope: a Sapce-Based Observatory for Extra-Solar Planet Detection," *Proc. 42nd Congress of the International Astronomy Federation*," Montreal, Oct. 1991.

3. S. Shaklan *et al.*, "Modeling of a Space-Based Ronchi Ruling Experiment for High-Precision Astrometry," submitted to *Astrophys. and Space Sci.*,, 1993.

4. D. Redding and W. Breckinridge, "Optical Modeling for Dynamics and Control Analysis,' *J.G.C.D.*, Vol 14, p. 1021, 1991.

5. G. N. Lawrence *et al.*, "High Accuracy Image Centroiding with a Moving Ronchi Ruling,' *Opt. Engineer.*, Vol. 30, p. 598, 1991.

6. Loral-Fairchild Imaging Sensors Catalog, 1991, part number CCD-481.

7. D. Korsch, in *The Astrometric Telescope Facility (ATF) FY'89 Final Report*, JPL pub. D-7113, p. 23, 1990.

8. J. Janesick *et al.*, "The Effects of Proton Damage on Charge-Coupled Devices," *Proc. SPIE 1447*, San Jose, 1991, p. 87.

9. T. Livermoore, private communication.